Optics Letters

Arithmetic logic unit based on the metastructure with coherent absorption

Jia-Hao Zou, Jun-Yang Sui, Qi Chen, and Hai-Feng Zhang*

College of Electronic and Optical Engineering & College of Flexible Electronics (Future Technology), Nanjing University of Posts and Telecommunications, Nanjing 210023, China
**hanlor@163.com*

Received 13 September 2023; revised 6 October 2023; accepted 6 October 2023; posted 10 October 2023; published 24 October 2023

An arithmetic logic unit (ALU) based on the metastructure (MS) with coherent absorption (CA) is proposed in this Letter. The ALU can perform AND and exclusive OR logical operations at the same frequency point. So it can be regarded as an optical half-adder. By controlling the chemical potential of graphene and the phase difference of coherent electromagnetic waves (EWs), two different binary numbers are input into the ALU. The dynamic absorption peaks, which are generated based on the CA, output the outcomes of the carry-digit bit and non-carry sum bit. This ALU can be used in the field of optical processing and encryption, such as processing hamming code. This given ALU based on the MS with CA has major implications for advancing the study and investigation into the application of CA. Furthermore, it also provides a new, to the best of our knowledge, idea for the study of MS with logical operation.

https://doi.org/10.1364/OL.505761

The arithmetic logic unit (ALU) is a logic device used to perform arithmetic. Half-adder is a crucial component of the ALU that performs addition operations. The inputs of a half-adder are typically denoted as X and Y, representing the binary digits to be added. The outputs consist of a carry bit (C) and a non-carry sum bit (S), which are obtained by, respectively, performing AND and exclusive OR (XOR) logical operations on the input bits. Half-adder is found in various applications in digital circuits, such as error detection and correction [1]. Optical ALU has the advantage of low power consumption and high computing efficiency [2]. With the development of quantum computing, the study of ALU with optical control is becoming significant [3].

Coherent absorption (CA) is a captivating research area within the field of optics because of its significant applications in light control and modulation [4,5]. By designing specific structures, researchers can attain highly selective absorption and modulation of electromagnetic waves (EWs). This technology holds an immense potential in areas such as optical devices [6], sensors [7], and logical operations [8]. In conventional scenarios, the ratio of absorption remains fixed. However, by precisely controlling the phase difference and amplitude ratio between the incident and reflected EWs, CA can be achieved. In addition, CA is a physically widespread phenomenon. So, it can be utilized in different kinds of materials and structures, including graphene [8] and metastructure (MS) [9].

As research for MS continues to advance, the MS with the function of logical operation is widely studied. Parandin *et al.* [10] designed an all-optical MS with the functions of NOR and AND logic gates based on the methods of finite difference time domain as well as plane wave expansion. Rao *et al.* [11] proposed a multiscale MS of magnetic-controlled AND logical operation based on the nonreciprocity of the magnetized InSb photonic structure. Sui *et al.* [12] put forward new ideas in the study of MS and designed an XOR logic gate based on metastructure, which are modulated by the external magnetic fields. These works are extremely important for the advancement of all-optical logic calculation, and they provide a unique idea for the research of MS. But these studies only realize the function of logical operations and do not extend to the ALU with the function of half-adder. Moreover, the MS with CA is rarely discussed in publications, especially having the same capabilities as half-adders.

In this Letter, an ALU based on the one-dimensional (1-D) MS with CA is given. Two separate binary integers are entered into the ALU by adjusting the chemical potential of graphene and the phase difference of coherent EWs. The results of both the C and S are output by the dynamic absorption peaks, which are created based on CA. So, it can realize the function of a half-adder. The proposed ALU provides a new idea for the application of CA in the field of quantum computing [2], photo-communication [3], and data processing and encryption [13].

The 1-D structure of the MS, which is depicted in Fig. 1, can be created by using the etching approach (Supplement 1 Section 1 introduces the specific process in detail). It is made up of ordinary A, B, and C dielectrics, air, and the combination layer (CL). Among them, dielectric A is barium strontium titanate (BST) doped by 10 wt% magnesium oxide (MgO), and the value of RI is $n_1 = n_2 = 16.49$ [14]. Titanium dioxide (TiO_2) and tellurium dioxide (TeO_2) are the respective components of dielectrics B and C, and their respective values of refractive index (RI) are 2.76 [15] and 2.4 [16], respectively. Two different CLs, which are respectively expressed as CL_1 and CL_2, are included in the MS. The CL_1 is located next to the outermost layer, and the CL_2 is right in the middle of the structure (see Fig. 1).

Every CL is staggered by graphene layer (GL) and silicon dioxide (SiO_2) like $SiO_2(GLSiO_2)^6$. The RI of SiO_2 is n_S, and

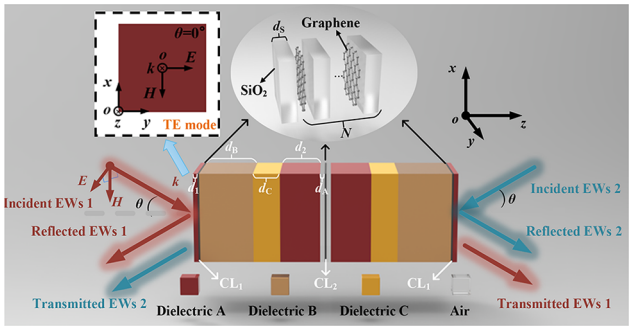

Fig. 1. Schematic diagram of the 1-D MS which is made up of different dielectric layers.

Table 1. Detailed Geometrical Dimensions of the MS

Parameters	d_1	d_2	d_A	d_B
Value	1 μm	9 μm	1 μm	12 μm
Parameters	d_C	d_S	N	θ
Value	6 μm	0.1 μm	6	0°

its value is 1.5 [17]. The thickness of GL is only the size of the diameter of a carbon atom molecule (0.34 nm) [18]. Moreover, the chemical potential μ_C of GL can significantly affect the RI of GL, and it can be controlled by modulating the external voltage (specific operation method is in Supplement 1 Section 2). In the case of no applied voltage, the chemical potential of graphene is 0.001 eV [5]. Because two different direct-current bias voltages will be applied, respectively, on CL_1 and CL_2, their chemical potentials which are regarded as ε_{C1} and μ_{C2} are different.

The entire construction is exposed to the air at the temperature of 270 K to study the general environment. d_i (i is indicated by 1, 2, A, B, C, S) expresses the thickness of dielectric layers. The incident EWs are located on the xoz plane and are refracted on the xoy plane. The angle between the EWs and the z axis in Fig. 1 is represented as θ (incident angle). The detailed geometrical dimensions of the structure are shown in Table 1. In addition, the theoretical model is the main focus of the study. Conventional mediums are unaffected by the external voltage, and the electronic band structure of the graphene is not affected by adjacent elements [19] (the detailed formulas are provided in Supplement 1 Section 3).

Since the longitudinal magnetic field component of the reaction is less, graphene mostly responds to the transverse electric field component. So, this work focuses on exploring the performance under a transverse electric (TE) mode. Under this mode, the electric field of EWs in Fig. 1 vibrates along the y axis, and the magnetic field vector is perpendicular to the plane formed by the y axis and the wave vector k. Only exploring the performance under the TE mode (the detailed formulas can be seen in Supplement 1 Section 4) can reduce the computational complexity and improve the computational efficiency while still capturing the main response characteristics of graphene.

Because the intensities of two coherent beams of EWs are the same, the equation about absorption (A) can be given as follows (Supplement 1 Section 5 has thorough information) [20]:

$$A = 1 - (|t| - |r|)^2 - 2|t||r|(1 + \cos\Delta\varphi_1\cos\Delta\varphi_2), \quad (1)$$

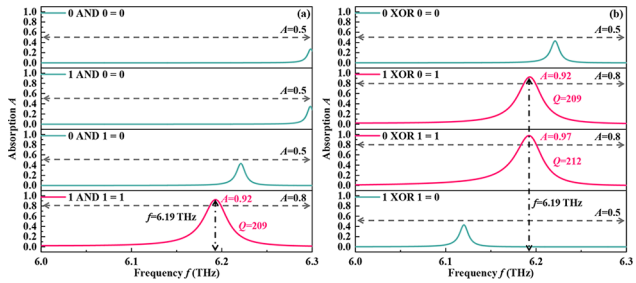

Fig. 2. Schematic diagrams of logical operations. (a) AND logic when the value of μ_{C1} is 0.001 eV. (b) XOR logic when the value of $\Delta\varphi_2$ is 0°.

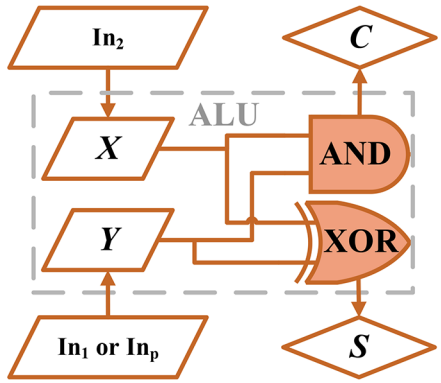

Fig. 3. Flow chart on the arithmetic logic process of the proposed ALU.

where t and r respectively express transmissivity and reflection coefficient, $\Delta\varphi_1 = \text{Arg}(t)\text{-Arg}(r)$ and $\Delta\varphi 2 = \varphi_+ - \varphi_-$. "Arg()" is used to represent the argument principal value of the plural.

According to the previously specified structural arrangement of the ALU, parameter A is calculated. A logic level (LL) of "1" is used to indicate chemical potential μ_C of GL in the case of 0.6 eV. Additionally, when the value of μ_C is 0.001 eV, it is denoted by the LL of "0." The phase difference $\Delta\varphi_2$ is denoted by the LL of "0" when its value is 180°. In the case of $\Delta\varphi_2 = 0°$, it is denoted by the LL of "1." An LL of "1" is used to indicate the formation of a sharp absorption peak (AP) when A is greater than 0.8. In the case of "$A < 0.5$," the LL is defined as "0." Figure 2 shows the schematic diagrams of logical operations (the more detailed simulation data is displayed in Supplement 1 Section 6). To evaluate the reliability of the ALU, the signal-to-noise ratio (SNR) is included. The formula is as follows [21]:

$$SNR(\text{dB}) = 10\log_{10}\left(\frac{A_1}{A_0}\right), \quad (2)$$

where A_1 and A_0 separately represent the value of A at an output value of "1" or"0" when the frequency point of EWs is 6.19 THz. SNR is larger than 3 dB which is regarded by engineers as the threshold between low and high SNRs [21].

The states of μ_{C2} and $\Delta\varphi_2$ are represented, respectively, by "In_2" and "In_p," and "Out" represents the presence of AP. The A spectra of realizing the AND logical operation under the condition of $\mu_{C1} = 0$ is displayed in Fig. 2(a). When the values of μ_{C2} and $\Delta\varphi_2$, respectively, are 0.001 eV and 0°, there is not a sharp AP and the A is smaller than 0.5. So, the states are "$In_2 = 0$," "$In_p = 0$," and "Out = 0," related to the "0 AND 0 = 0" of the

Table 2. Truth Value Table of the AND and XOR Logic Gates

AND	In_2	In_p	Out
$SNR = 9.6$ dB	0 ($\mu_{C2} = 0.001$ eV)	0 ($\Delta\varphi_2 = 180°$)	0 ($A < 0.5$)
	1 ($\mu_{C2} = 0.6$ eV)	0 ($\Delta\varphi_2 = 180°$)	0 ($A < 0.5$)
	0 ($\mu_{C2} = 0.001$ eV)	1 ($\Delta\varphi_2 = 0°$)	0 ($A < 0.5$)
	1($\mu_{C2} = 0.6$ eV)	1($\Delta\varphi_2 = 0°$)	1($A > 0.8$)
XOR	**In_1**	**In_2**	**Out**
$SNR = 9.6$ dB	0($\mu_{C1} = 0.001$ eV)	0($\mu_{C2} = 0.001$ eV)	0($A < 0.5$)
	1($\mu_{C1} = 0.6$ eV)	0($\mu_{C2} = 0.001$ eV)	1($A > 0.8$)
	0($\mu_{C1} = 0.001$ eV)	1($\mu_{C2} = 0.6$ eV)	1($A > 0.8$)
	1($\mu_{C1} = 0.6$ eV)	1($\mu_{C2} = 0.6$ eV)	0($A < 0.5$)

Table 3. Truth Value Table of the Arithmetic Logic Process

Condition	X (In_2)	Y (In_p)	C
$\mu_{C1} = 0.001$ eV	0	0	0
	1	0	0
	0	1	0
	1	1	1
Condition	**X (In_2)**	**Y (In_1)**	**S**
$\Delta\varphi_2 = 0°$	0	0	0
	1	0	1
	0	1	1
	1	1	0

AND logic gate. When $\mu_{C2} = 0.6$ eV and $\Delta\varphi_2 = 0°$, a sharp AP is not formed and the A is smaller than 0.5. The same thing happens when $\mu_{C2} = 0.001$ eV and $\Delta\varphi_2 = 180°$. Therefore, the states can be expressed by "1 AND 0 = 0" and "0 AND 1 = 0." When the values of μ_{C2} and $\Delta\varphi_2$ are, respectively, 0.6 eV and 180°, a sharp AP forms and the value of A is larger than 0.8 ($A = 0.92$). The frequency corresponding to the AP is 6.19 THz, and the value of the quality factor (Q) is 209. The states are "$In_2 = 1$," "$In_p = 1$," and "Out = 1," related to the "1 AND 1 = 1" of the AND logic gate. The terms "In_1" and "In_2" refer to the states of the μ_{C1} and μ_{C2}, respectively.

As shown in Fig. 2(b), the A spectra of realizing the XOR logical operation under the condition of $\Delta\varphi_2 = 0°$. When both the values of μ_{C1} and μ_{C2} are 0.001 eV and 0.6 eV, the value of A is smaller than 0.5. So, the states can be represented by "0 XOR 0 = 0" and "1 XOR 1 = 0." When one of the values of μ_{C1} and μ_{C2} is 0.6 eV, and the other is 0.001 eV, there is a sharp AP, and the value of A is larger than 0.8 ($A = 0.92$ or $A = 0.97$). The frequencies corresponding to the APs are 6.19 THz, and their values of Q are respectively 209 and 212. Under these conditions, the states can be represented by "1 XOR 0 = 1" and "0 XOR 1 = 1." As shown in Fig. 2, the frequency points of APs ($A > 0.8$) are the same. This demonstrates that the ALU can perform AND and XOR logical operations at the same frequency point. Additionally, the relatively high values of Q can illustrate that the results calculated by the ALU are receivable. The truth value table belongs to the AND and XOR logic gates as shown in Table 2. Supplement 1 Section 7 offers a way to obtain the value of A. The flow chart and logic process of ALU can be seen in Fig. 3 and Table 3, respectively.

To more clearly analyze the propagation of EWs in the ALU and explain the reasons for AP forming, Fig. 4 (based on the code of FDTD), which contains two electric field intensity distribution maps, is plotted. As can be seen in Fig. 4, when the

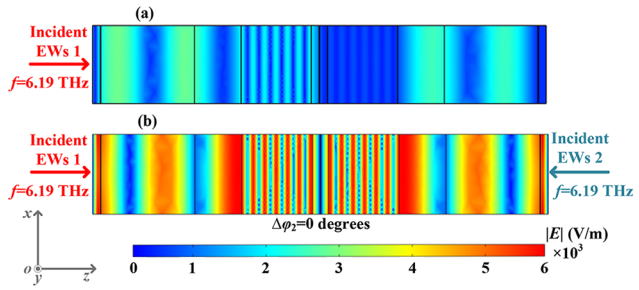

Fig. 4. Electric field intensity distribution maps when the frequency of EWs is 6.19 THz, μ_{C1} is 0.001 eV and μ_{C2} is 0.6 eV. (a) Incident EW 1 exists, but incident EW 2 does not. (b) Both incident EW 1 and incident EW 2 exist, and $\Delta\varphi_2$ is 0°.

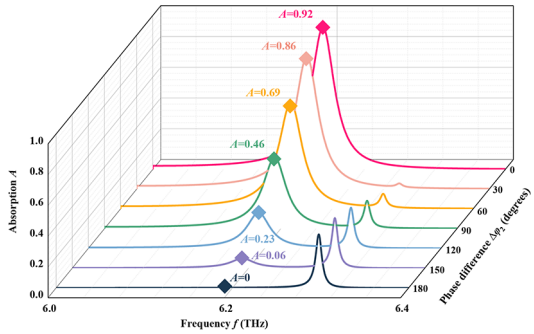

Fig. 5. Effect of different $\Delta\varphi_2$ on the value of A at 6.19 THz.

frequency of EWs is 6.19 THz, μ_{C1} is 0.001 eV and μ_{C2} is 0.6 eV. Because GLs are introduced into the ALU as defect layers and the ALU is constructed of layered media, there are local defects and interface effects, which make the electric field energy concentrated between two CLs. Furthermore, when two beams of EWs are relative incident, as can be observed in Fig. 4(b), the electric field intensity is larger than it is in the case of only one beam of incident EWs, whose electric field intensity distribution is illustrated in Fig. 4(a). The higher the intensity of the electric field, the stronger the interaction will be between the EWs and the electrons or molecules in the medium [10]. Thus, the A of EWs in the ALU increases when the frequency point is 6.19 THz. This proves that by CA, the value of A can be significantly improved and receive a good result.

The phase difference $\Delta\varphi_2$ between the two beams of incident EWs is one of the important influencing factors for the result of CA. Figure 5 displays the effects of different $\Delta\varphi_2$ on the value of A at 6.19 THz. At the range of 0–180°, the maximum value of AP continually declines as $\Delta\varphi_2$ improves. The maximum AP, which can enhance the quality of the ALU, is generated when the value of $\Delta\varphi_2$ is 0° and the value of A is 0.92. However, when the value of $\Delta\varphi_2$ is 180°, the value of A at 6.19 THz drops down to 0. Because of these, the phase differences of 0 and 180° are regarded separately as two different input LLs. Furthermore, different chemical potential μc denoting as the LL of "1" also is able to influence the results of APs and the quality of the ALU.

Figure 6 demonstrates the difference in the APs under the different cases of μ_C. When the value of μc is in the range of 0.4–0.6 eV, which can be seen in Fig. 6(a), as the value of μ_C is continually increasing, the frequency point difference value Δf between the two APs belonging to the case of different LLs is shrinking down. When the value of μc is 0.6 eV, the value

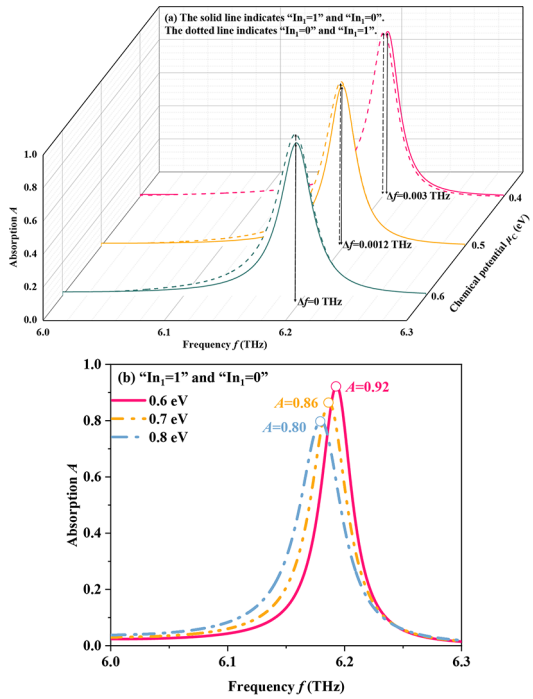

Fig. 6. Effect of different μ_C denoting as the LL of "1" on the APs. (a) The APs about different μ_C (the values of μ_C are 0.4, 0.5, and 0.6 eV) when the two input LLs are different. (b) The APs about different μ_C (the values of μ_C are 0.6, 0.7, and 0.8 eV) in the case of "$In_1 = 1$" and "$In_2 = 0$."

Table 4. Published Reports Compared with the Proposed ALU in Terms of the Performance

Refs.	SNR (dB)	Logic Operation	CA	Arithmetical Operation	1-D MS
[10]	×	AND and NAND	No	No	No
[11]	9.5	AND	No	No	Yes
[12]	9.7	XOR	No	No	Yes
[22]	×	AND and OR	No	No	No
[23]	4.5	AND and XOR	No	Half-adder	No
This work	9.6	AND and XOR	Yes	Half-adder	Yes

of Δf becomes 0 THz, which can improve the computational efficiency and accuracy of the ALU. The effect of different μ_C in the range of 0.6–0.8 eV on the APs in the case of "$In_1 = 1$" and "$In_2 = 0$" is shown in Fig. 6(b). Under the condition of "$In_1 = 1$" and "$In_2 = 0$," the A of AP is dwindling constantly as the value of μ_C is continually increasing. Because the reduction of A will make the detection of AP more difficult, the performance of the ALU will deteriorate. In addition, the higher μc means that more electric energy is used to stimulate CLs. Thus, the power dissipation of the ALU will increase, and more energy will be wasted. Period number N also has a certain impact on ALU performance (the detailed analysis process is in Supplement 1 Section 9).

According to the research discussion above, the ALU proposed in this Letter has excellent performance, which can satisfy the needs of half-adder based on CA. To logically and methodically show the benefits of the proposed ALU, Table 4 lists some related works done before and compares the ALU with them.

In conclusion, the proposed MS can be regarded as an ALU with CA. By controlling the chemical potential of graphene and the phase difference of coherent EWs, two separate binary integers can be input into the ALU. Through observing the case of absorption peaks, the ALU can calculate the outcomes of C and S like a half-adder. As can be seen in Table 4, the ALU based on the 1-D MS with CA has major implications for advancing study and investigation into the application of CA. It also provides a new way for the research of ALU with optical control. Moreover, what needs to be emphasized is that due to the limitation of funds and experimental conditions, experimental verification cannot be carried out. So, this Letter focuses on theoretical innovation and demonstrates the point of view of simulation. All the results in this Letter have been recognized before and are calculated through the software which are recognized by the industry. So, the results in this Letter are valid.

Disclosures. The authors declare no conflicts of interest.

Data availability. Data underlying the results presented in this paper are not publicly available at this time but may be obtained from the authors upon reasonable request.

Supplemental document. See Supplement 1 for supporting content.

REFERENCES

1. R. W. Hamming, The Bell Syst. Tech. J. **29**, 147 (1950).
2. V. Venkataraman, K. Saha, and A. L. Gaeta, Nat. Photonics **7**, 138 (2013).
3. M. Santagiustina, S. Chin, and N. Primerov, *et al.*, Sci. Rep. **3**, 1594 (2013).
4. W. Wan, Y. Chong, and L. Ge, *et al.*, Science **331**, 889 (2011).
5. S. Zanotto, F. Bianco, and V. Miseikis, *et al.*, APL Photonics **2**, 016101 (2017).
6. A. Xomalis, I. Demirtzioglou, and E. Plum, *et al.*, Nat. Commun. **9**, 182 (2018).
7. Y. R. Wu, R. Y. Dong, and J. H. Zou, *et al.*, Phys. Chem. Chem. Phys. **25**, 14257 (2023).
8. R. Ebrahimi Meymand, A. Soleymani, and N. Granpayeh, Opt. Commun. **458**, 124772 (2020).
9. R. Alaee, Y. Vaddi, and R. W. Boyd, Opt. Lett. **45**, 6414 (2020).
10. F. Parandin and M. M. Karkhanehchi, Superlattices Microstruct. **101**, 253 (2017).
11. S.-S. Rao, J.-T. Zhang, and H.-F. Zhang, Results Phys. **31**, 105058 (2021).
12. J.-Y. Sui, Y.-M. Liu, and H.-F. Zhang, Waves in Random and Complex Media **1**, 1 (2023).
13. X.-H. Song, H.-Q. Wang, and S. E. Venegas-Andraca, *et al.*, Phys. A **537**, 122660 (2020).
14. F. Zhang, S. Feng, and K. Qiu, *et al.*, Appl. Phys. Lett. **106**, 091907 (2015).
15. J. R. DeVore, J. Opt. Soc. Am. **41**, 416 (1951).
16. N. Uchida, Phys. Rev. B **4**, 3736 (1971).
17. I. H. Malitson, J. Opt. Soc. Am. **55**, 1205 (1965).
18. A. K. Geim, Science **324**, 1530 (2009).
19. A. Andryieuski and A. V. Lavrinenko, Opt. Express **21**, 9144 (2013).
20. W. Zhu, F. Xiao, and M. Kang, *et al.*, Appl. Phys. Lett. **108**, 121901 (2016).
21. D. H. Johnson, Scholarpedia **1**, 2088 (2006).
22. Z. Guan, W. Li, and W. Ding, *et al.*, in *Proceedings of 2011 IEEE Pacific Rim Conference on Communications, Computers and Signal Processing* (2011), pp. 925–931.
23. Y. Pugachov, M. Gulitski, and O. Mizrahi, *et al.*, Symmetry **15**, 1063 (2023).